Fabrication-tolerant, 2-mode, 4λ multiplexer based on Si waveguides for beyond Tbit/s optical Ethernet

Takeshi Fujisawa and Kunimasa Saitoh
Graduate School of Information Science and Technology, Hokkaido University North 14, West 9, Kita-ku, Sapporo 060-0814, Japan
Email: fujisawa@ist.hokudai.ac.jp

Abstract: A fabrication-tolerant, 2-mode, 4λ multiplexer is proposed for beyond Tbit/s optical Ethernet system. Various techniques for strengthening fabrication tolerance are introduced, and a proof-of-concept device is fabricated for Si-photonics platform. © 2023 The Author(s)

1. Introduction

To cope with the rapid increase of data traffic between and within data centers, 400GbE has been standardized in 2017 [1]. There are several standards, which use wavelength-division-multiplexing (WDM) technology, to increase the capacity. For example, four and eight wavelengths are used in 400GBASE-LR4 and -LR8. In the transmitter for these systems, wavelength multiplexer (λ MUX) is necessary. Variety of λ MUXs [2-5] were proposed, and among them, λ MUX based on Si-photonics platform is a promising candidate for their compactness and mass productivity. For the future high-speed Ethernet, Tbit/s transmission will be required. For achieving Tbit/s, increasing the number of wavelengths is one possibility. For the 4λ MUXs, two-stage Mach-Zehnder (MZ) MUXs are suitable option. The problem of the two-stage MZ MUXs is the controllability of peak wavelength position. A slight deviation in the arm waveguide width and delay line length of MZ filters results in the peak wavelength fluctuation. Therefore, there is a limit in the number of wavelengths for cascaded MZ filters. An arrayed waveguide grating (AWG) is suitable for the λ MUX with large number of wavelengths, however, AWGs based on Si waveguides are relatively high loss. Since the cost of the device is very important for Ethernet device, strong fabrication tolerance is primary important to increase the yield of the device.

A mode-division-multiplexing (MDM) technique has attracted a lot of attentions to increase the capacity of optical fiber transmission system. By using MDM, since we can increase the network capacity with another dimension, it is not necessary to increase the number of wavelengths. Especially, MDM is suitable for chip-based transmission link, such as optical interconnect. To utilize MDM, a mode multiplexer (mode MUX) is necessary. For Si-photonics platform, there are a lot of mode MUXs and an asymmetric directional coupler (ADC) is one of the most promising candidate for the mode MUX. However, the fabrication tolerance of normal ADCs is not so strong, and the bandwidth is limited. Therefore, to utilize MDM with WDM in Si-photonics platform, a broadband and fabrication-tolerant mode MUX is strongly desired.

In this paper, we propose and experimentally demonstrate fabrication-tolerant, 2-mode, 4λ MUXs on Si-photonics for future Tbit-scale Ethernet systems, including chip-based optical interconnect. For the mode MUX, we fabricated tapered ADC designed by wavefront matching (WFM) method [6,7] for the first time. The measured characteristics exhibit broadband, low-loss, and fabrication-tolerant spectra, which is favorable for cost-effective Ethernet system. For the 4λ MUXs, two techniques are introduced for strengthening the fabrication tolerance: fabrication-tolerant delay line design [8], and 2 × 2 and 2 × 1 MZ filter configuration to lock the peak wavelength position between two MZ filters [5]. A proof-of-concept device is fabricated and fabrication-tolerant characteristics in terms of waveguide width variation is demonstrated. By using recently developed ultrahigh-speed light source, such as 100G-PAM4 [9], the proposed MUX can be used for Tbit-scale Ethernet systems.

2. Device design and results

The left panel of Fig. 1 shows the schematic of the device. The device consists of one 2-mode MUX and two 4λ MUXs. The 2-mode MUX is a WFM-designed ADC (WFMADC), as shown later. The 4λ MUX is a two-stage MZ MUX. It consists of two 1st MZ filters and one 2nd MZ filter. The free spectral range (FSR) of 2nd MZ filter is half of 1st MZ filters. One of the 1st MZ filter is 2 × 2 configuration and the other is 2 × 1 configuration. The schematic of the 2 × 2 MZ filter is shown in the right panel of Fig. 1. First MZ filter multiplex two wavelengths and second MZ filter multiplex four wavelengths. We used MPW service to fabricate the device, and the microscope picture of the entire device is shown in the middle panel of Fig. 1, which has one input port and 8 output ports (Ports 1 to 8).

We used standard SOI substrate with the Si-core thickness of 220 nm. Upper cladding is silica. First, we explain the design of mode MUX. The left upper panel of Fig. 2 shows the schematic of the tapered ADC. It consists of tapered bus waveguide and access waveguide. The bus waveguide has trapezoidal shape, and the waveguide width is tapered from w_{bin} =820 nm to w_{bout} = 860 nm. The width of access waveguide is w_{acc} = 400 nm. The separation between two waveguides is *gap* = 200 nm. TE0 mode launched to the access waveguide is converted to TE1 mode in the bus waveguide. As stated above, the mode MUX should be broadband, low-loss, and fabrication-tolerant. These features are especially important for Ethernet device because the cost of the device is very important. To achieve all of these features by human design is a little bit difficult, and therefore, we used the WFM method, which is a kind of inverse design. By using WFM method, the waveguide width is automatically modulated to achieve the desired characteristics. The detail of the algorithm was demonstrated elsewhere [6]. From our experience, since it is not favorable to modulate the waveguide width of multimode waveguide, we only modulate one side of the access waveguide as shown in Fig. 2. The final structure of the top-view of the WFMADC and the microscope of the fabricated device are shown in the left-bottom panel of Fig. 2. The right panel of Fig. 2 shows the calculated (dashed) and the measured (solid) transmission spectra of the single WFMADC fabricated on the same chip. For the measurements, TE light is launched through the inverse taper spot-size converter and output light is measured by optical spectrum analyzer. To show the fabrication tolerance, we fabricated device patterns, whose waveguide widths are intentionally changed by ±10 nm (Δw = ±10 nm) from ideal design (Δw = 0 nm). The mode conversion loss (TE0 to TE1) is about 1-dB over the measured wavelength range, and almost independent in terms of the waveguide width variation. Calculated results agree well with those of measured spectra, and as shown in the Figure, broadband and fabrication-tolerant transmission spectra are obtained.

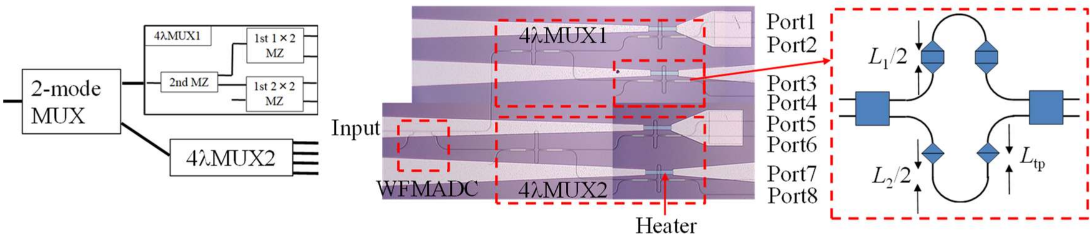

Fig. 1 (Left) The schematic of the device. (Middle) a microscope picture of the fabricated device. (Right) a schematic of MZ filter.

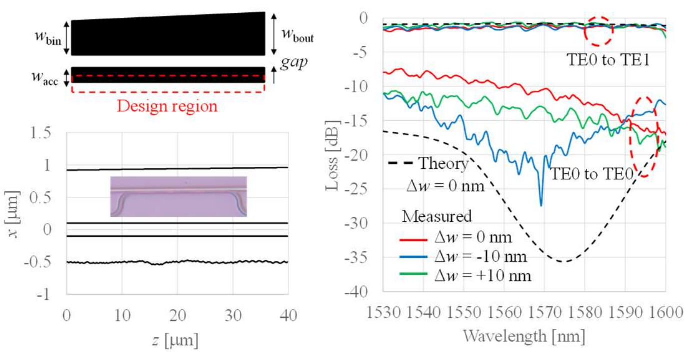

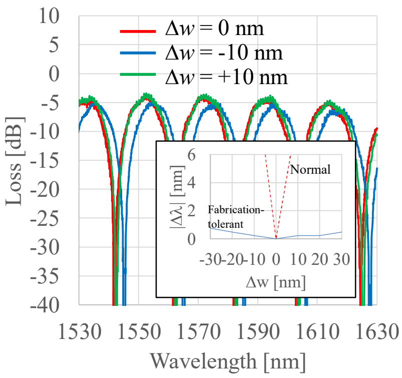

Fig. 2 (Left up) the schematic of tapered ADC. (Left bottom) WFM-designed ADC outline and microscope picture of the fabricated device. (Right) Calculated and measured transmission spectra of WFMADC.

Fig. 3 Measured transmission spectra of fabrication-tolerant MZ filters with the FSR of 20 nm. The inset shows calculated peak wavelength shift as a function of waveguide width deviation.

Next, we explain the design of 4λ MUX. The biggest problem of two-stage MZ MUX is the controllability of the peak wavelength position. Here, we used two techniques to resolve the problem. First is to use the fabrication-tolerant delay line design. As shown in the right panel of Fig. 1, the tapered waveguide is introduced in the delay line waveguides. The waveguide width before and after the taper are w_2 and w_1. L_1 and L_2 are defined in the Figure. By satisfying following condition, the peak position variation in terms of the waveguide width is greatly suppressed.

$$\frac{dn_{eff,1}}{dw}L_1 - \frac{dn_{eff,2}}{dw}L_2 = 0 \qquad (1)$$

where, $n_{\mathrm{eff}1,2}$ are the effective indexes of the waveguide with the widths of w_1 and w_2. These parameters are set for desired FSR. For Tbit-scale system, although the wavelength spacing has not been standardized yet, we tentatively set FSR = 40 and 20 nm for first and second MZ filters (10-nm wavelength spacing). For these FSRs, we set w_1 = 400 nm and w_2 = 600 nm. L_1 and L_2 are 22.4 and 7 µm for FSR = 40 nm, and 45.2 and 14.2 µm for FSR = 20 nm to satisfy (1). The length of the taper waveguide L_{tp} = 50 µm. The inset in Fig. 3 shows calculated peak wavelength variations $|\Delta\lambda|$, as a function of waveguide width deviation Δw, for MZ filter with the FSR of 20 nm. The dashed line is for normal MZ filter with the waveguide width of 400 nm, and the solid line shows the one for fabrication-tolerant design. The effect is obvious and fabrication-tolerant design gives much stronger fabrication tolerance. Fig. 3 shows the measured transmission spectra of the designed 2 × 2 MZ filter with the FSR of 20 nm for different waveguide width, fabricated on the same chip. For Δw = +10-nm width deviation, the spectra are almost unchanged compared with that of Δw = 0 nm, and for -10-nm width deviation, the spectra is shifted by 2 to 3 nm, which is much smaller than conventional design, as shown in the inset. The losses of MZ filters are relatively high. This is probably because of non-optimized 3-dB couplers (MMI) and can be reduced much by optimizing it.

Second feature to strengthen the fabrication-tolerance is to use 2 × 2 and 2 × 1 MZ filter configuration for 1st MZ filters. By using 2 × 1 MZ filter, the peak wavelength position is locked exactly at the center of two adjacent peak wavelengths of 2×2 MZ filter due to the π/2-phase difference [5]. Figure 4 shows that the normalized measured transmission spectra of single 2 × 2 and 2 × 1 MZ filters with the FSR of 20 nm, fabricated on the same chip. The peak positions of 2 × 1 MZ filter are nearly at the center of 2 × 2 MZ filters. This configuration eliminates the adjustment of the length of the delay line waveguides between first MZ filters.

Finally, we measured the transmission of 2-mode, 4λ MUX, shown in Fig. 1. We measured DMUX characteristics by launching light from the Input. For the measurement of 4λ MUX2, we have to excite TE1 mode to couple at the WFMADC. Therefore, we fabricate one more WFMADC at the input port (not shown in Fig. 1), and light is launched from the access waveguide of the WFMADC to convert TE0 to TE1 mode. Since the peak positions of 1st and 2nd MZ filter may not be matched, microheaters are placed on top of the delay line waveguides of 1st MZ filters and used to tune the spectra, as shown in Fig. 1. Figure 5 shows the normalized transmission of proposed MUX. Currents are injected to microheaters and the values are 50, 47, 35, and 30 mA for MZ filters of Port1-2, Port3-4, Port5-6, and Port7-8, respectively. The averaged loss is -7 dB for Ports 1 to 4 and -9.3 dB for Ports 5 to 8. Since for Ports 5 to 8, the light has passed WFMADC (1-dB loss) two times, 2-dB increase is reasonable. The relatively high loss comes, again, from non-optimized 3-dB couplers, as shown in Fig. 3, and can be reduced much by optimizing the components. Clear and very low crosstalk spectra are obtained for all the ports, showing the usefulness of the proposed device.

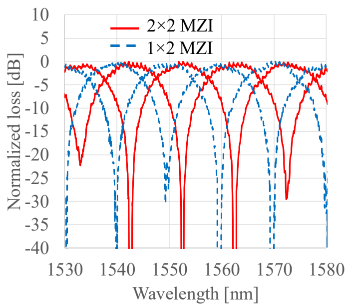

Fig. 4 Measured normalized transmission spectra of 2 × 2 and 2 × 1 MZ filters.

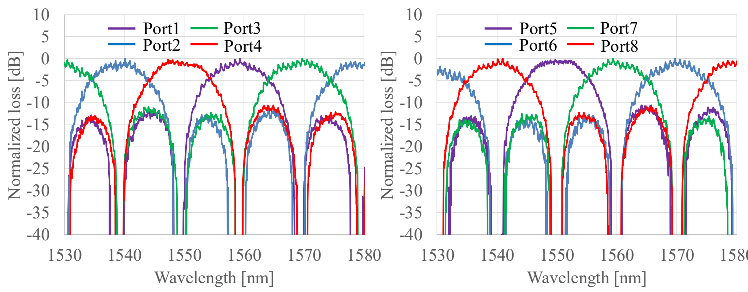

Fig. 5 Measured normalized transmission spectra of 2-mode, 4λ MUX. (Left) Ports 1 to 4 (TE0 mode). (Right) Ports 5 to 8 (TE1 mode).

3. Conclusion

We proposed fabrication-tolerant, 2-mode, 4λ MUXs on Si-photonics for future Tbit-scale Ethernet systems. Various techniques, such as inverse designed mode MUX, fabrication-tolerant delay line design, and 2 × 2 and 2 × 1 MZ filter configuration, are employed to strengthen the fabrication tolerance of the MUX, which is very important for Ethernet device. The proof-of-concept device is fabricated and clear mode/wavelength multiplexing operation is demonstrated.

4. Reference

[1] http://www.ieee802.org/3/bs/
[2] T. Akiyama, et al., Proc of OFC2018, W1l.2 (2018).
[3] K. Hassan *et al*., *Opt. Lett.*, **40**, 2641–2644 (2015).
[4] L. Chang *et al*., *IEEE PTL*., **29**, 1237–1240 (2017).
[5] T. Fujisawa et al., JLT, **39**, 193 (2021).
[6] Y. Sawada, et al., Opt. Exp., 29, 27322 (2021).
[7] Y. Sawada et al., JLT, 36, 3652 (2018).
[8] T.-H. Yen et al., JLT, 39, 146 (2021)
[9] S. Kanazawa et al., Proc of OFC2016, Th5B.3 (2016).